4D microtomography of brine-assisted healing processes in deformation-damaged rocksalt

Y. Ji[1], C. J. Spiers[1], S.J.T. Hangx [1], J.H.P. de Bresser[1], M.R. Drury [1]*

[1]Department of Earth Sciences, Utrecht University, the Netherlands;

** y.ji@uu.nl*

ABSTRACT:

Rock salt formations represent key options for storage of natural gas, hydrogen and compressed air energy, and for storage or disposal of radioactive waste. Undisturbed rock salt deposits are ually impermeable and have very low porosity. However, as a result of cavation, near-field microcracking and associated dilatancy occur in rock salt, increasing porosity and permeability. The connectivity of a brine- or water-vapour-filled microcrack network in deformation-damaged salt, is expected to decrease over time, partly due to dissolution-precipitation healing. Here, we employ 4D (i.e. time-resolved 3D) microtomography to study the long-term evolution of dilated grain boundary and microcrack networks developed in deformation-damaged natural salt by such brine-assisted processes. We found substantial microstructural modification or healing over periods of days to a few months. Cracks and dilated grain boundaries became crystallographically faceted, necked, discontinuous and disconnected, and often migrated to “recrystallize” the material, producing an increase in tortuosity and a decrease in connectivity of the crack network. The magnitude and rate of associated permeability reduction and its evolution with time remain to be determined in future studies.

1 Introduction

By virtue of its low permeability d high ductility, rock salt has long been identified as a favorable host rock for solution-mined oil and gas storage caverns and for conventionally mined radioactive waste repositories (e.g. Langer 1993, 1999). Driven by the growing urgency to transition to non-fossil energy sources, current interest in salt is also fast expanding towards construction and re-use of solution-mined caverns for large scale storage of hydrogen and compressed air energy.

To evaluate the long term performance and safety of all such systems, and of abandoned salt-production caverns, a quantitative understanding is needed of the coupled mechanical behavior and transport properties of salt. Extensive experimental data exist on the creep behavior of intact salt rock (e.g. Carter et al. 1993; Hunsche and Hampel 1999), on the development and mechanical closure of microcrack damage (Alkan et al., 2007) and on compaction creep of salt backfill material (Hansen et al., 2014). These have been cast into constitutive models that are widely applied in geomechanical simulations of storage system and repository behavior (e.g. Hampel et al. 2010). The predictions of such simulations are crucial for evaluating the timescale for closure and ultimate sealing (to natural salt

permeabilities) of boreholes and backfilled openings, for example. Not yet included, however, are the effects of crack and pore healing by dissolution-precipitation processes. These are known to occur in salt when small amounts of brine or adsorbed water are present and are expected to dominate permeability reduction in the late stages of convergence of boreholes and backfilled cavities, i.e. when deviatoric and effective mean stresses and associated strain rates are low (Houben et al., 2013). They may also play a role in controlling permeability evolution under the low deviatoric and effective stress conditions expected in the roof region abandoned brine caverns.

Under such conditions, the connectivity and contiguity of brine-filled or water-film-coated grain boundaries, triple junctions, pores and microcracks present in deformation-damaged or granular salt are expected to decrease over time by internal mass transfer involving dissolution, diffusion and precipitation of salt - at least up to fluid pressures (P) of around 75 MPa and temperatures (T) around 100℃ (Lewis and Holness, 1996). The driving force for this type of healing process is the tendency to reduce the total interfacial energy by reducing the salt-brine interfacial area, in the approach to an equilibrium state defined by characteristic dihedral wetting angles at salt-salt contacts. Provided porosity lies below a geometric threshold of 4-5% determined by the equilibrium dihedral angle for the salt-brine system (Ghanbarzadeh et al., 2015) such healing processes are expected to cause a slow decrease in the permeability of salt, depending on pressure-temperature conditions.

The progress of these dissolution-precipitation processes has been directly observed over periods of a few days in cleavage-crack healing experiments performed on single crystals of NaCl in an optical cell, at room temperature and pressure with controlled relative humidity (Houben et al., 2013). Crack contraction rates measured in these experiments demonstrated that healing was controlled by diffusion through adsorbed water/brine films. Similar optical observations have been made on grain boundary healing in static annealing experiments on deformed potash salts (Urai 1987; Schenk and Urai 2004). Pore reconfiguration by dissolution-precipitation transfer is also implied by the end results of fully hydrostatic experiments on granular salt plus brine mixtures performed by Lewis & Holness (1996) and Ghanbarzadeh et al. (2015), in which mean dihedral angles were measured, after hydrostatic annealing at elevated P-T conditions for several days. These studies respectively employed petrographic imaging and ray micro-computed tomography (μCT). Advanced μCT imaging (Cnudde & Boone, 2013; Ji et al., 2015) has also been applied to the characterization of pore and inclusion arrays in natural rocksalt (Thiemeyer et al. 2014, 2015; Burliga and Czechowski 2010) and to timelapse imaging of fine, granular salt undergoing compaction creep by pressure solution (e.g. Renard et al. 2004; Macente et al. 2018). However, we know of no μCT imaging work on the long term progress of crack healing and pore reconfiguration by solution transfer processes in either coarse granular salt (e.g. backfill) or in plastically deformed and dilated salt rock of the type expected in the walls of converging openings.

In this paper, we report a series of novel healing experiments performed on plastically pre-deformed and dilated (cracked) samples of coarse natural rock salt, using time-lapse μCT imaging. Our goal was to capture evidence for the healing processes operating under brine-saturated, room P-T conditions, over times up to 3 months, and to obtain insight into the progress and rate of these processes.

2 Methodology

2.1 General approach

The present experiments were conducted on natural polycrystalline rocksalt at room temperature and atmospheric pressure. Small samples were mechanically deformed, damaged and dilated under unconfined conditions, flooded with saturated brine and hermetically sealed. In this way, newly generated cracks and dilated grain boundaries were exposed to saturated salt solution and subject to the effects of dissolution, diffusion, and precipitation. The healing process thus initiated was imaged at different stages (in time-lapse mode employing increasing time intervals) using an X-ray CT microscope (μCT tests), as illustrated in Figure 1.

2.2 Sample preparation for CT imaging - specifics

Polished cylinders of Leine rocksalt (Leinesteinsalz from the German Zechstein, grain size [illegible] mm) measuring 3.5-5 mm diameter and 7-15 mm length were first deformed in unconfined axial compression to create microcrack damage alongside [illegible] to 7% of plastic deformation. The microcrack dilatancy obtained corresponded to several percent of intergranular crack and grain boundary porosity, with occasional transgranular cracks also being present. The deformed samples were then jacketed in an FEP (fluorinated ethylene propylene) heat-shrink sleeve and CT scanned in the lab-dry condition. The sample-jacket assembly was then suction-flooded with saturated brine and located in a PEEK (polyether ether ketone) polymer capsule or “bottle”. The vessel-sample assembly was subsequently sealed by adding a rubber sheet and plug, as gaskets, and a screw-on PEEK closure-lid. In the mm thickness range used for [illegible]nstructing the PEEK vessels, PEEK is essentially X-ray transparent, allowing maximum resolution to be obtained, in conjunction with the small sample dimensions. The sample assembly and associated components used are illustrated in Figure 2.

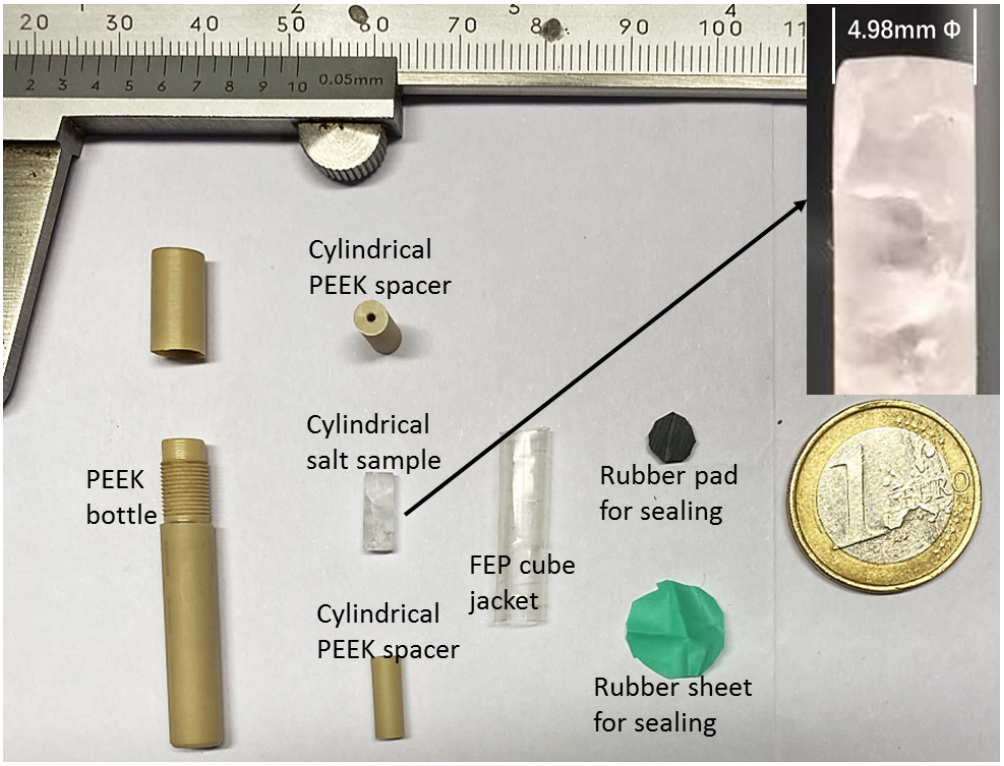

Figure 2: Sample assembly used for µCT. Note the cylindrical rocksalt sample of 4.98mm diameter and the accessories needed to encapsulate the sample for scanning in the brine-saturated condition. In the upper right corner is an enlarged view of the sample.

2.3 X-ray Computed Microtomography

Healing experiments were conducted on six deformed/cracked rocksalt samples. CT imaging was performed using a ZEISS Xradia 610 Versa 3D X-ray Microscope located in the Multi-scale Imaging and Tomography Facility (MINT) at Utrecht University. Multiple series of projections were acquired for each sample. The number of projections per scan was varied from 2001 to 4501 to achieve a high signal-to-noise ratio within acceptable scanning duration. Image reconstructions were done using the "Reconstructer Scout-and-Scan" software developed by Zeiss, employing pixel sizes ranging from 0nm to 7µm. We used incident X-rays generated using a voltage of 50 kV and 6.5 W power, combined with a source filter to optimize the transmittance of the projection images. As a result, the grey level contrast between solid salt grains, saturated brine and air was maximized and clearly distinguishable in the reconstructed images.

To capture the evolution of healing in each sample studied, a series of CT scans was performed on each sample at gradually increasing time intervals (timelapse imaging). A first scan was conducted on each sample before brine addition, i.e. on the deformed/ cracked, dry sample. The second scan was conducted immediately after brine-flooding and capsule sealing. Subsequent scans of wet samples were performed at gradually increasing time intervals from one day, three days, one week, one month, and up to 3 months. By doing so, we managed to

capture the 4D (i.e. time-resolved 3D) healing process occurring in the damaged rocksalt samples.

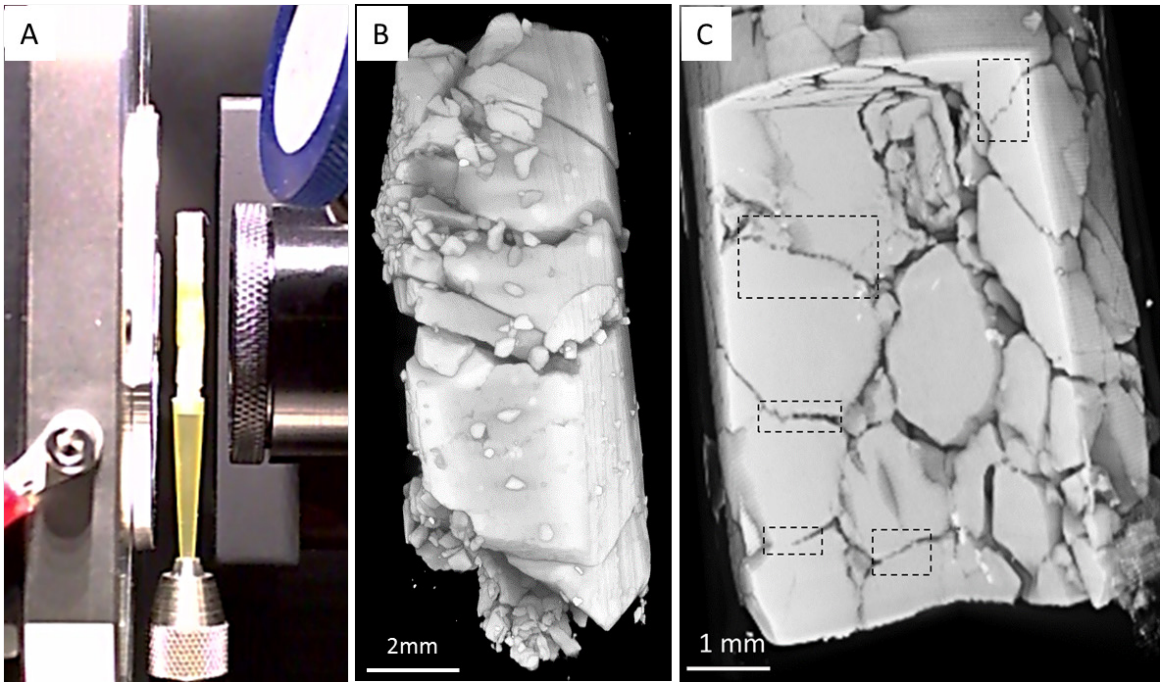

Figure 1, Use of µCT to image a rock salt sample. (A) A FEP-jacketed rock salt cylinder (5 mm diameter) being scanned in X-ray CT microscopy. (B) Typical 3D CT image of a cracked salt sample (dry). (C) Reconstructed CT image obtained 13 days after driving saturated brine through a deformation-damaged salt cylinder; note the inter-, intra- and transgranular cracks.

3 Results

The CT imaging results obtained are illustrated below in Figures 3 to 5. Undeformed samples showed intact grains and undilated grain boundaries decorated with fluid inclusions (Figure 3A). Old, healed cracks were also visible. Samples that were deformed only and not (yet) impregnated with saturated brine showed wide, sharply defined grain boundary cracks, and occasional intra- and nsgranualr cracks, that were clearly connected throughout the samples, providing high permeability pathways (Figure 3B). No change was observed in these microstructural features in samples that were stored in a dry environment, at least over periods up to five months. After introducing brine, the microstructure started to change and a wide variety of healing phenomena were observed. In the first a few days, we saw a change in surface roughness on the outside of the samples. Their smooth, polished, outer surface became irregular or wavy, with an amplitude of 0.05 to 0.2 mm within a few weeks (Figure 5).

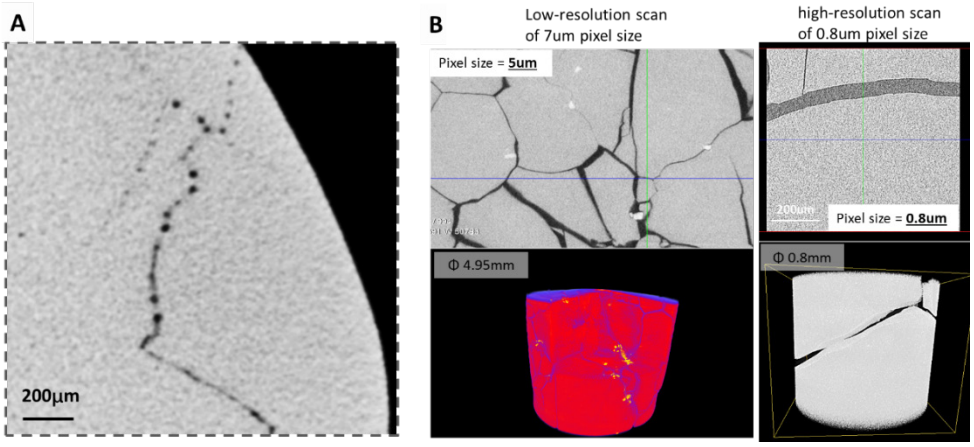

Figure 3: µCT images showing the undeformed Leine rocksalt starting material (A) and axially compressed samples (B) and (C). (A) Grain boundary with fluid inclusions in the undeformed starting material. Healed cracks also visible. (B) Intergranular and transgranular cracks formed after axial deformation of samples XLSS02, but before brine addition and the onset of healing processes. (C) A subvolume in (B) using a zoom-in scan high resolution (800nm) CT scan.

Within one day of adding brine and on-going in the subsequent days and weeks, we observed widespreak crystallization, overgrowth and surface reconfiguration within the defomation-induced cracks and pores. Some grains grew topotactically into adjacent pores and cracks, or “ate into” their neighbours by grain boundary migration (i.e. migration of dilated grain boundaries and cracks), forming stepped, idomorphic (100) cube faces in both cases (Figures 4 and 5). As healing time increased further, most of the deformation-induced cracks and deformation-dilated grain boundaries became more tortuous. This was due to a) the development and progressive coarsening of a zig-zag morphology reflecting the tendency for migrating boundaries and open crack walls to adopt stepped, low energy (100) crystal forms, and b) an accompaying tendency for dilated boundaries and cracks to neck down into less well-connected arrays of pores and inclusions, often as the (001) steps growing on opposing crack walls impinged upon each other (Figures 4 to 6). Significant crack and pore reconfiguration was observed over periods of 2-3 weeks, with major changes occurring in the longest runs (3 months), which showed markedly increased tortuosity and reduced (2D) connectivity (Figures 4 - 6).

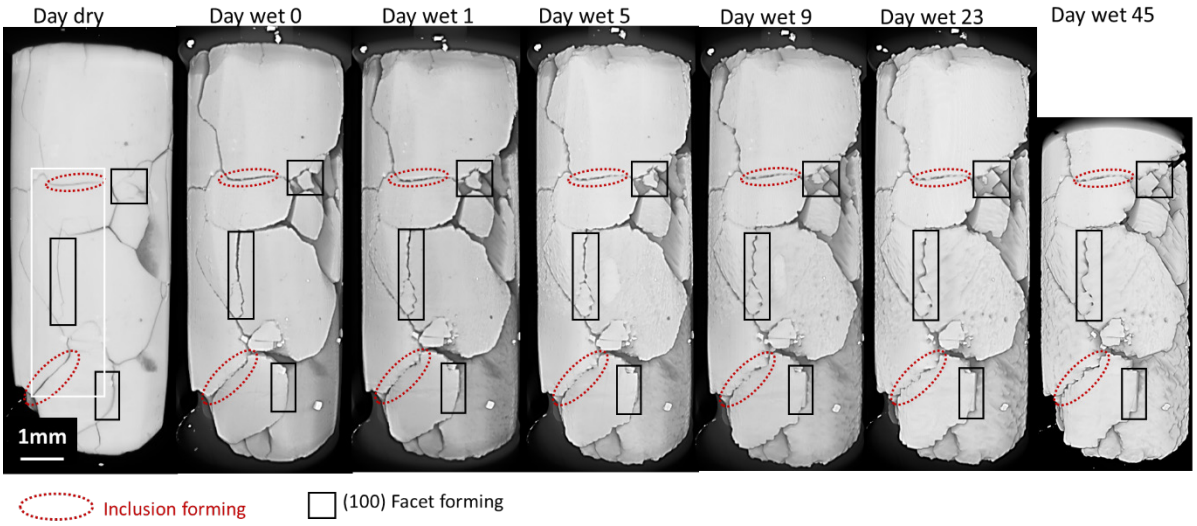

Figure 4: µCT images showing evolution of the crack network in a pre-cracked samples over 45 days of healing. Sample number XLLS006. Salt is in grey, voids (pores and cracks) are in black. Red dashed ellipses mark the regions with cracks are becoming disconnected and inclusions are being formed. Black rectangles show regions of grain boundary (or crack) migration. These data show clear modification and disconnection of the crack network over time, inevitably resulting in a decrease in permeability. Over the maximum test duration of 3 months, even larger changes were observed.

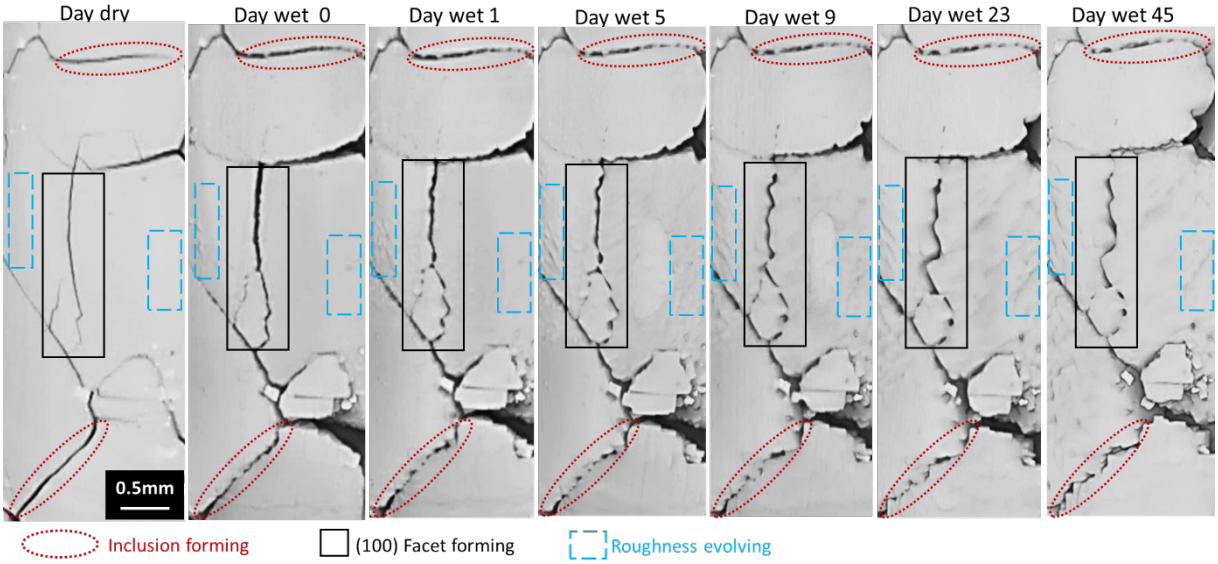

Figure 5: Enlargement of the subregion marked with the white rectangle in Figure 4.Salt is grey, voids (pores and cracks) are black. Red dashed ellipses mark dilated, brine-filled grain boundaries that are becoming disconnected due to necking down of the fluid film to form and island-channel structure and ultimately isolated inclusions. Black rectangles show sites of marked crack migration with local necking of the internal fluid film to form more isolated inclusions (lower portion). Blue rectangles mark the area of roughness evolving.

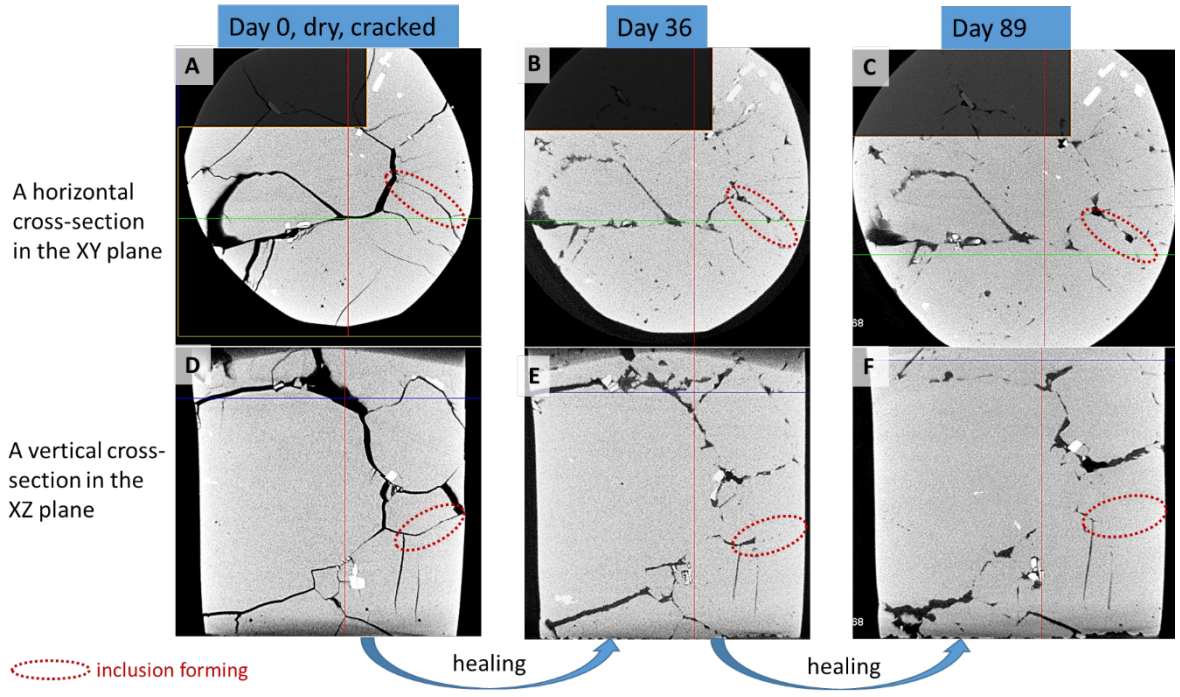

Figure 6. Reconstructed CT images showing crack network evolution in a deformation-damaged rock salt sample in the initial dry condition (left), after 36 days of healing following brine addition (center), and after 89 days of healing (right). Sample number XLLS005. Salt in grey, voids (pores and cracks) in black. (A), (B) (C) are horizontal cross-sections orientated normal to the cylindrical sample axis. (D), (E), (F) are vertical cross-sections orientated parallel to the cylindrical sample exis. Red dashed ellipses mark regions containing cracks that are becoming disconnected due to the formation of inclusion arrays. Local grain/interface boundary migration is also visible.

4. Discussion and Conclusions

This study has reported high-resolution X-ray CT imaging of the evolution of grain boundary and microcrack healing processes occurring in stically deformed and microcrack-magedrocksalt under brine saturated conditions. The experiments were conducted at room temperature and pressure over periods up to 3 months, with the aim of elucidating the dissolution-precipitation processes that are believed to dominate crack/pore healing and permeability reduction in salt when deviatoric and effective mean stresses are low, e.g. in the late stages of convergence of boreholes and backfilled cavities.

We observed several phenomena in the CT tests, after addition of brine. Besides roughening of the outer surfaces of the samples, idiomorphic (100) topotactic overgrowths developed on the walls of larger pores and wide cracks. Other dilated grain boundaries and trans/intragranular cracks served as sites for migration of the brine-filled boundary or crack such that one side advanced at the expense of the other, again with idiomorphic (100) forms dominating Perhaps most importantly from the perspective of permeability reduction, most cracks, both grain boundary and intra/transgranular, became more tortuous and less well connected with healing time, due to the development of a (100)-controlled, zig-zag, surface-

step morphology combined with step impingement and necking down of the internal fluid film to form (incipient) inclusion arrays.

.

This necking down of dilated grain boundaries and cracks to form (incipient) inclusion arrays is qualitatively consistent with the results of the crack healing experiments on cleaved single crystals of NaCl reported by Houben et al. (2013) and with the concept of surface area/ energy reduction by dissolution-precipitation transfer. The topotactic overgrowth features and (100) steps or faceting that we observed on dilated grain boundary and trans/intragranular crack surfaces, which did not show wholesale migration, were presumably caused by local surface energy minimization over crack walls. In other words, initially irrational, high energy crystallographic (crack) surfaces became reconfigured into stepped (100) surfaces, which have the minimum surface energy in NaCl (Bruno et al., 2009). issolution step of this process y also have been enhanced by release of dislocation-stored strain energy induced by the plastic deformation suffered by the samples. In the case of grains consuming portions of their neighbours, we infer that strain-induced boundary migration involving dissolution-precipitation transfer across dilated grain boundaries and cracks occurred, driven by differences in dislocation stored energy related to plastic deformation, with surface energy minimization or kinetic factors again favouring the formation of (100) surfaces at migrating interfaces. This follows from direct comparison with brine-assisted grain boundary migration seen in dense rock salt deforming by dislocation mechanisms under confined, non-dilatant conditions (Urai *et al.*, 1986; Peach et al., 2001; Ter Heege et al., 2005; Pennock et al., 2006).

Conceptual models put forward by previous researchers (e.g. Houben et al., 2013) predict that crack healing should produce isolated or only partly connected pores with reduced surface area, by two processes: i) dissolution and precipitation driven by surface area/energy reduction, and ii) growth of new, strain free crystals (grain boundary migration) over pre-existing brine-filled cracks, again by dissolution-precipitation phenomena but driven by release of stored dislocation strain energy. Our experimental results show clear evidence that both of the above mechanisms substantially modify the pore, crack and grain microstructure of the deformed and dilated salt within a few weeks to months.

We note that (100) faceting of migrating interfaces was ch more prevalent than observed in the studies of equilibrium dihedral angle development in the salt-brine system, as a function of P and T (up to 200 °C and 200 MPa), reported by Lewis & Holness (1996) and Ghanbarzadeh et al. (2015). These authors equilibrated loose, fine salt (analytical reagent, 0.2-0.4 mm grain size cubes) with brine, at zero Terzaghi effective stress, and obtained a sintered microstructure of well-rounded grains and well-defined dihedral angles. By contrast, equilibrium was clearly not reached in our experiments as the microstructure continued to evolve even after 2-3 months. We infer that this reflects the lower temperature, coarser grain size and wider pore/crack spacing (i.e. slower diffusion rates) characterizing our experiments, as well as the fact that our samples were plastically deformed (i.e. charged with dislocation-stored energy) and not subjected to intial grain dissolution and “rounding” by heating to elevated temperatures. The implication is that the equilibrium state seen in the above dihedral angle experiments cannot be reached without total recrystallization of our samples - or perhaps not at all due to the intervention of some intermediate meta-stable equilibrium state

characterized by local equilibrium in the pore network only. This draws the applicability of previous equilibrium diahedral angle data to plastically deformed and dilated salt rock into question regarding the prediction of pore connectivity in deformed rock salt. The applicability of the mean dihedral angle data reported by Lewis and Holness (1996) to the computation of pore connectivity (i.e. of the percolation threshold) and permeability is also open to question purely because the strong anisotropy of surface energy evidenced in our experiments is not accounted for (e.g. Laporte and Provost, 2000).

We suggest that studies of plastically deformed and dilated/cracked rock salt samples can better simulate the evolution and final healed state of crack and grain boundary networks, as developed in the walls of converging galleries and boreholes, than mean dihedral angle perimenbts on synthetic granular samples. Our results show that, in the early stage of healing, relatively planar, brine-filled grain boundary and trans/intragranular cracks become more tortuous due to (100)- controlled overgrowth and grain boundary migration by dissolution-precipitation transfer. Cracks and dilated grain boundaries become crystallographically stepped, necked/irregular, discontinuous and disconnected, and can migrate to “recrystallize” the material. The associated increase in tortuosity and decrease in connectivity and contiguity of the fluid pathways within dilated grain boundaries and cracks must concomitantly reduce crack network permeability. However, the magnitude and rate of permeability reduction and its evolution with time remain to be determined.

Though incomplete, the present results indicate that substantial healing occurs in stically deformed and dilated/damaged rock salt in periods of weeks to months at room temperature, when brine saturated. They offer a starting point for development and testing of new microphysical-thermodynamic models for healing by dissolution-precipitation processes and are expected to be relevant not only to plastically deformed and dilated rocksalt but also to plastically compacted salt backfill. In future, we plan to conduct experiments with longer healing times to capture the formation of inclusions and the further disconnection of the crack network. We also plan to conduct CT experiments at higher temperatures and effective stress states that better simulate the conditions in converged boreholes, backfilled openings and salt cavern walls. A crucial further step will be to determine the permeability evolution that accompanies the dissolution-precipitation healing, either by direct measurement or by fluid dynamics computation (Arns et al., 2004) based on CT characterization of the evolving crack and grain boundary network.

Acknowledgements

This study was sponsored by the Dutch TopSector programme, TKI project (TKI2017-08-UG). The CT instrument at the Multi-scale Imaging and Tomography Facility (MINT) at Utrecht University was funded by the Netherlands Research Council (NWO) via the EPOS-NL Research Infrastructure programme.

References

Alkan, H., Cinar, Y., Pusch, G., 2007. Rock salt dilatancy boundary from combined acoustic emission and triaxial compression tests. Int. J. Rock Mech. Min. Sci. 44, 108–119.

Arns, C.H., Knackstedt, M.A., Pinczewski, W.V., Martys, N.S., 2004. Virtual permeametry on

microtomographic images. J. Pet. Sci. Eng. 45, 41–46.

Bruno, M., Aquilano, D., Prencipe, M., 2009. Quantum-Mechanical and Thermodynamical Study on the (110) and Reconstructed (111) Faces of NaCl Crystals. Cryst. Growth Des. 9, 1912–1916.

Burliga, S., Czechowski, F., 2010. Anatomy of hydro-carbon-bearing zones, hydrocarbon provenance and their contribution to brittle fracturing of rock salt in the Klodawa Salt Structure (central Poland), in: Solution Mining Research Institute Spring 2010 Technical Conference. pp. 125–134.

Carter, N.L., Horseman, S.T., Russell, J.E., Handin, J., 1993. Rheology of rocksalt. J. Struct. Geol. 15, 1257–1271. https://doi.org/https://doi.org/10.1016/0191-8141(93)90168-A

Ghanbarzadeh, S., Hesse, M.A., Prodanović, M., Gardner, J.E., 2015. Deformation-assisted fluid percolation in rock salt. Science (80-.). 350, 1069–1072.

Hampel, A., Gunther, R.M., Salzer, K., Minkley, W., Pudewills, A., Leuger, B., Zapf, D., Staudtmeister, K., Rokahr, R., Herchen, K., Wolters, R., Lux, K.-H., Schulze, O., Heemann, U., Hunsche, U., 2010. Benchmarking of Geomechanical Constitutive Models For Rock Salt. 44th U.S. Rock Mech. Symp. 5th U.S.-Canada Rock Mech. Symp.

Hansen, F.D., Popp, T., Wieczorek, K., St, D., 2014. Salt Reconsolidation Principles and Application. Sandia National Lab.(SNL-NM), Albuquerque, NM (United States).

Houben, M.E., ten Hove, A., Peach, C.J., Spiers, C.J., 2013. Crack healing in rocksalt via diffusion in adsorbed aqueous films: Microphysical modelling versus experiments. Phys. Chem. Earth, Parts A/B/C 64, 95–104.

Hunsche, U., Hampel, A., 1999. Rock salt — the mechanical properties of the host rock material for a radioactive waste repository. Eng. Geol. 52, 271–291.

Langer, M., 1999. Principles of geomechanical safety assessment for radioactive waste disposal in salt structures. Eng. Geol. 52, 257–269.

Langer, M., 1993. Use of solution-mined caverns in salt for oil and gas storage and toxic waste disposal in Germany. Eng. Geol. 35, 183–190.

Laporte, D., Provost, A., 2000. Equilibrium geometry of a fluid phase in a polycrystalline aggregate with anisotropic surface energies: Dry grain boundaries. J. Geophys. Res. Solid Earth 105, 25937–25953. https://doi.org/https://doi.org/10.1029/2000JB900256

Lewis, S., Holness, M., 1996. Equilibrium halite-H2O dihedral angles: High rock-salt permeability in the shallow crust? Geology 24, 431–434.

Macente, A., Fusseis, F., Butler, I.B., Tudisco, E., Hall, S.A., Andò, E., 2018. 4D porosity evolution during pressure-solution of NaCl in the presence of phyllosilicates. Earth Planet. Sci. Lett. 502, 115–125.

Renard, F., Bernard, D., Thibault, X., Boller, E., 2004. Synchrotron 3D microtomography of halite aggregates during experimental pressure solution creep and evolution of the permeability. Geophys. Res. Lett. 31.

Schenk, O., Urai, J.L., 2004. Microstructural evolution and grain boundary structure during static recrystallization in synthetic polycrystals of Sodium Chloride containing saturated brine. Contrib. to Mineral. Petrol. 146, 671–682.

Thiemeyer, N., Habersetzer, J., Peinl, M., Zulauf, G., Hammer, J., 2015. The application of high resolution X-ray computed tomography on naturally deformed rock salt: Multi-scale investigations of the structural inventory. J. Struct. Geol. 77, 92–106.

Thiemeyer, N., Pusch, M., Hammer, J., Zulauf, G., 2014. Quantification and 3D visualisation of pore space in Gorleben rock salt: constraints from CT imaging and microfabrics.

Zeitschrift der Dtsch. Gesellschaft für Geowissenschaften 165, 15–25.

Urai, J.L., 1987. Development of microstructure during deformation of carnallite and bischofite in transmitted light. Tectonophysics 135, 251–263.

Urai, J.L., Spiers, C.J., Zwart, H.J., Lister, G.S., 1986. Weakening of rock salt by water during long-term creep. Nature 324, 554–557.